

N 62 70835

NASA TN D-261



7N-20  
198525  
P-37

# TECHNICAL NOTE

D-261

## ONE-DIMENSIONAL ANALYSIS OF ION ROCKETS

By Harold R. Kaufman

Lewis Research Center  
Cleveland, Ohio

NATIONAL AERONAUTICS AND SPACE ADMINISTRATION

WASHINGTON

March 1960

(NASA-TN-D-261) ONE-DIMENSIONAL ANALYSIS OF  
ION ROCKETS (NASA) 37 p

N89-70473

Unclas  
00/20 0198525

NASA TN D-261

NATIONAL AERONAUTICS AND SPACE ADMINISTRATION

---

TECHNICAL NOTE D-261

---

ONE-DIMENSIONAL ANALYSIS OF ION ROCKETS

By Harold R. Kaufman

SUMMARY

A one-dimensional analysis was made of space-charge effects in ion and electron accelerators and the problems associated with mixing beams from such accelerators. The results of the analysis were examined to determine some of the major design problems and performance limitations of ion rockets.

Heavy ions were found to be particularly desirable for high current density when ion-accelerator lengths are limited by manufacturing tolerances rather than dielectric strength. The accelerate-decelerate principle also helps to offset the effect of minimum electrode spacing on ion current density.

The similar geometrical design of electron and ion accelerators leads to excessive electron velocities or exit areas, or both, probably even when the accelerate-decelerate principle is utilized for the electron accelerator. Excessive electron velocities cause only part of the electron current to go downstream when neutralization is attempted. High electron velocities can be utilized, however, if the total electron current is large enough that the electron current transmitted is sufficient to neutralize the ion beam.

The high-electron-velocity mixed-beam solutions are accompanied by upstream electron currents; therefore, the ion accelerator must be able to withstand electrons bombarding the exit. The accelerate-decelerate principle is also useful for preventing harm to the ion accelerator due to this electron bombardment, because the electrons will be unable to pass through the field between the accelerating and decelerating electrodes to reach the ion source.

INTRODUCTION

The concept of electrical space propulsion is not new. The accepted initial reference for the concept is reference 1, a book by Oberth published in 1929. Subsequent technical advances in electric powerplants

spurred further study of electrical propulsion as shown in references 2 and 3. For example, nuclear-electric powerplant weights of the order of 10 pounds per kilowatt appear feasible. As shown in reference 3, electrical propulsion with such a powerplant has the potential of transporting large payloads in space with gross weights at least as small as those of any competitive system.

The overall program for the investigation of the ion thrust unit, or ion rocket, at the NASA Lewis Research Center is presented in reference 4. A derivation of the thrust equation and application to a one-dimensional ion rocket with grid neutralization is presented in reference 5.

This report is limited to a one-dimensional analysis of space-charge effects in ion and electron accelerators and the problems associated with mixing beams from such accelerators. The results of the analysis are examined to determine some of the major design problems and performance limitations of ion rockets. Although accurate application of the results is limited to those designs which approximate one-dimensionality, the qualitative results are expected to be applicable to more general design configurations.

#### SYMBOLS

A	atomic weight per electronic charge
E	potential gradient or electric field, volts/meter
$\bar{E}$	mean electric field, volts/meter
F	thrust, newtons, (kilogram)(meter)/sec <sup>2</sup>
g	dimensional constant, 9.807 meters/sec <sup>2</sup>
I	specific impulse, sec
J	current (positive for positive particles and negative for negative particles), amp
j	current density (positive for positive particles and negative for negative particles), amp/meter <sup>2</sup>
k	Boltzmann constant, $1.380 \times 10^{-23}$ joules/(°K)(molecule)
m	particle mass, kilograms
$\dot{m}$	mass-flow rate, kilograms/sec

$n$	number density, meter <sup>-3</sup>
$n_0$	total number of particles per cubic meter, meter <sup>-3</sup>
$\dot{n}$	number rate, sec <sup>-1</sup>
$q$	charge, coulombs
$S$	cross-sectional area, meters <sup>2</sup>
$T$	temperature, °K
$V$	potential, volts
$V'$	particle thermal potential, volts
$\bar{V}$	mean thermal potential (potential of particle at $\bar{v}$ ), volts
$v$	particle velocity, meters/sec
$v'$	particle thermal velocity, meters/sec
$\bar{v}$	most probable velocity of Maxwellian distribution, meters/sec
$x$	distance, meters
$\beta$	$(4\epsilon_0/9)/\sqrt{2q/m}$
$\epsilon_0$	dimensional constant, $8.855 \times 10^{-12}$
$\lambda$	wavelength, meters
$\rho_q$	charge density, coulombs/meter <sup>3</sup>

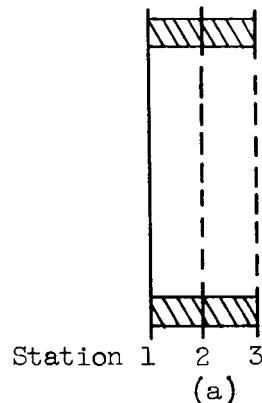
Subscripts:

$a, b,$ $c, d$	indices
$av$	average
$E$	station E, zero-electric-field plane
$e$	emitted
$eq$	equivalent (equivalent electron potential gives electron velocity equal to ion velocity)

i	ideal (ideal thrust assumes immediate neutralization at exit of ion accelerator)
min	minimum
N	station N, neutralization plane
r	reference station for measuring potential difference
t	transmitted
tot	total
1	station 1, particle source
2	station 2, acceleration electrode
3	station 3, deceleration electrode
+	ion
-	electron

#### ANALYSIS

An ion rocket has accelerators for both positive and negative particles. A schematic diagram of an accelerator is shown in sketch (a):



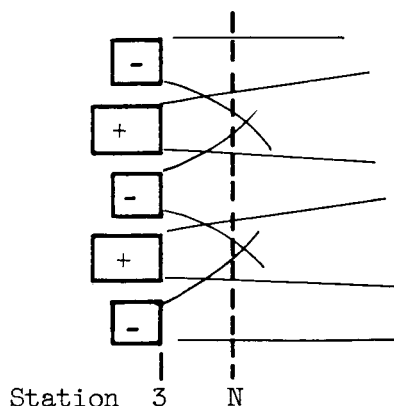
The plane of particle emission is designated station 1. Station 2 is an accelerating electrode. A decelerating electrode will often be of use and is designated station 3 when used. Since the decelerating potential difference is always less than the accelerating potential difference, the charged particles can escape from the accelerator. A zero electric field, when it is found at some plane other than one of the stations

noted, is referred to as station 1E or 2E, depending on what station it follows. The distance in the direction of particle motion is measured by the variable  $x$ . The distance between stations 1 and 2 is therefore  $x_2 - x_1$ . The potential difference between two stations is given in a similar manner by  $V_3 - V_2$ .

The requirement of one-dimensionality is met by having constant-area beams with conditions uniform on each plane normal to the direction of motion and the motion restricted to one direction. These requirements may be met in practice by using parallel screens for electrodes and having the beam width large compared to the distance between stations, or it might be met by using a narrow beam with contoured electrodes outside the beam such as suggested by Pierce. The electrodes were also assumed to be good shields so that the space charge on one side of an electrode would not affect a charged particle on the other side.

Since equal magnitudes of negative and positive beam currents are necessary, both forms of accelerators are used in a complete ion rocket. The positive particles are assumed to be ions, while the negative ones are assumed to be electrons. Negative ions could be used in place of electrons, but the added complexity (and weight) of another ion source makes this solution undesirable.

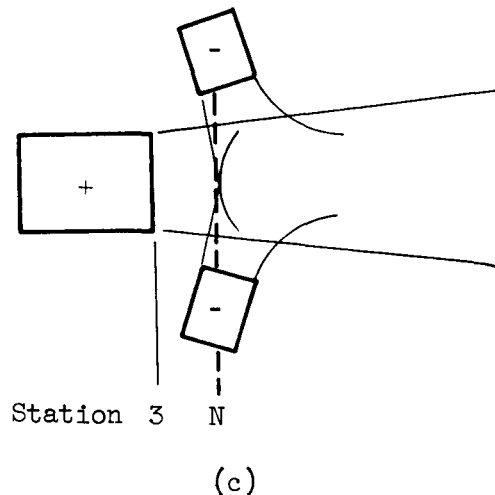
Several arrangements of electron and ion accelerators might be used. An array of small electron and ion accelerators might be used in the same plane, as shown in sketch (b):



(b)

The electron beams would spread into the ion beams so that neutral beams are effectively obtained at the neutralization plane, station N, which is the distance  $x_N - x_3$  downstream of the accelerator exits. The

configuration of sketch (b) may depart considerably from the one-dimensional neutralization plane; in which case only approximate agreement with analysis would be expected. Another configuration that might fit the one-dimensional requirement is the single-unit ion rocket shown in sketch (c):



The region between station 3 and station N may cause substantial deceleration of the ions and therefore might be substituted for the deceleration region between stations 2 and 3. The exit of the accelerator in either sketch (b) or (c) would then be station 2.

It should be apparent that a large number of component arrangements are possible. A deceleration region may be desired on either the ion or electron accelerator, but not on the other accelerator; and the deceleration region may be inside an accelerator or outside. Some means of eliminating the unpromising configurations is obviously of interest. To carry this elimination all the way down to "one best design," however, would be premature at present.

The approach in this report is more modest. The component regions common to all configurations are considered one at a time: the acceleration region (stations 1 to 2), the internal deceleration region (stations 2 to 3), the external deceleration region (from the accelerator exit to the electron-injection or neutralization plane, station N), and finally a mixed electron-ion beam region downstream of station N. The one-dimensional space-charge effects in each of these regions are examined with regard to overall ion-rocket performance and problems. Thus, the general results are in terms of a few overall design principles and limits. These principles and limits can be used to eliminate some of the many possible configurations, but the number of configurations remaining will be sufficient to offer ample challenge for further work in the field.

The space-charge effects in each of the regions are found by solving Poisson's equation in one dimension, which is

$$\frac{d^2V}{dx^2} = - \frac{\rho_q}{\epsilon_0} \quad (1)$$

in the units of the rationalized mks system. The charge density  $\rho_q$  can be expressed in terms of current density  $j$  and velocity  $v$  for the case of uniform velocity at each station:

$$\rho_q = \frac{j}{v} \quad (2)$$

The velocity can in turn be obtained from energy considerations:

$$v = \sqrt{2(V_r - V)(q/m)} \quad (3)$$

with the potential difference  $V_r - V$  measured so that the velocity is zero when the difference is zero.

Substituting equations (2) and (3) into (1),

$$\frac{d^2V}{dx^2} = - \frac{j}{\epsilon_0 \sqrt{2(V_r - V)(q/m)}} \quad (4)$$

Equation (4), then, is one form of Poisson's equation used in this report.

For problems dealing with both positive and negative particles, the charge density of equation (1) can be evaluated as a sum of the positive and negative charge density. Using equations (2) and (3), Poisson's equation for this case becomes

$$\frac{d^2V}{dx^2} = - \left[ \frac{j}{\epsilon_0 \sqrt{2(V_r - V)(q/m)}} \right]_- - \left[ \frac{j}{\epsilon_0 \sqrt{2(V_r - V)(q/m)}} \right]_+ \quad (5)$$

If a distribution of particle velocities is involved, integration will be required to calculate the charge density:

$$\frac{d^2V}{dx^2} = - \int_0^j \frac{dj}{\epsilon_0 \sqrt{2(V_r - V)(q/m)}} \quad (6)$$

This form of Poisson's equation will be discussed in more detail in the section on Maxwellian distribution.

## Acceleration Region

The usual ion-acceleration region between stations 1 and 2 has the boundary condition of zero initial velocity. The same boundary condition can be applied in an approximate fashion to stations 1 and 2 in an electron accelerator, although the thermal motion will be found important for electrons. Using the equations for the acceleration region, the performance of accelerators without any decelerating electrodes and the need for an accelerate-decelerate system can be shown.

Child's law. - Space-charge-limited current with zero initial velocity gives the boundary conditions at station 1 of

$$\frac{dV}{dx} = 0$$

$$v = 0$$

Integrating equation (4) from  $V_1$  to  $V_2$  and from  $x_1$  to  $x_2$  with these boundary conditions yields the solution

$$j = \left(\frac{4\epsilon_0}{9}\right) \sqrt{\frac{2q}{m}} \frac{(V_1 - V_2)^{3/2}}{(x_2 - x_1)^2} \quad (7)$$

This solution was first obtained by Child in 1911 (ref. 6) and is usually associated with his name.

Making a substitution of

$$\beta = \frac{4\epsilon_0}{9} \sqrt{\frac{2q}{m}} \quad (8)$$

to simplify the symbols in equation (7),

$$j = \beta \frac{(V_1 - V_2)^{3/2}}{(x_2 - x_1)^2} \quad (9)$$

The constants in equation (3) and (9) were evaluated in mks units and are tabulated as follows:

Quantity	Electrons	Ions
$\sqrt{2q/m}$	$5.932 \times 10^5 i$	$1.389 \times 10^4 / \sqrt{A}$
$\beta$	$2.334 \times 10^{-6} i$	$5.467 \times 10^{-8} / \sqrt{A}$

where  $A$  is the atomic weight per electronic charge, or simply the atomic weight for singly ionized ions, and  $i$  is the square root of  $-1$  (resulting from the negative charge of electrons).

Thrust and mean electric field. - The ideal thrust (the thrust that would be obtained with neutralization immediately downstream of the accelerator) can be related directly to the potential gradient in the accelerator. The ideal thrust per unit beam area is

$$\frac{F_i}{S} = \dot{m} \frac{v_i}{S} = \dot{m} \frac{v_2}{S} \quad (10)$$

The mass flow per unit area is

$$\frac{\dot{m}}{S} = j \frac{m}{q} \quad (11)$$

Substituting equation (11) into (10),

$$\frac{F_i}{S} = j v_2 \frac{m}{q} \quad (12)$$

Substituting the velocity and current-density expressions (eqs. (3) and (7)) into (12) gives

$$\frac{F_i}{S} = \frac{8\epsilon_0}{9} \frac{(V_1 - V_2)^2}{(x_2 - x_1)^2} \quad (13)$$

Noting that the mean electric field  $\bar{E}$  is equal to  $(V_1 - V_2)/(x_2 - x_1)$ , equation (13) may be rewritten

$$\frac{F_i}{S} = \frac{8\epsilon_0}{9} \bar{E}^2 \quad (14)$$

Finally, evaluating the constants in mks units,

$$F_i/S = 7.871 \times 10^{-12} \frac{\bar{E}^2}{\text{newtons/meter}^2} \quad (15)$$

Thus, the ideal thrust per unit beam area can be considered a function of the mean electric field and independent of particle velocity or charge-to-mass ratio. The maximum electric field is, of course, greater than the mean value, but the factor is only  $4/3$  for the ideal one-dimensional case considered.

Practical limits. - Practical limits on the electric field should be considered before drawing conclusions from equations (14) or (15). The limits on the electric field to which insulators should be subjected are from about  $10^6$  to  $10^7$  volts per meter, while high field electron

emission (with subsequent arcing) occurs at about  $10^8$  to  $10^9$  volts per meter. These are local and not mean values, so that electrode designs incorporating sharp edges and corners would arc-over at a lower mean electric field than  $10^8$  or  $10^9$  volts per meter. Gaseous breakdown through the ion beam need not be considered, because space-charge limitations result in particle densities too low to permit electron cascades and gaseous discharges.

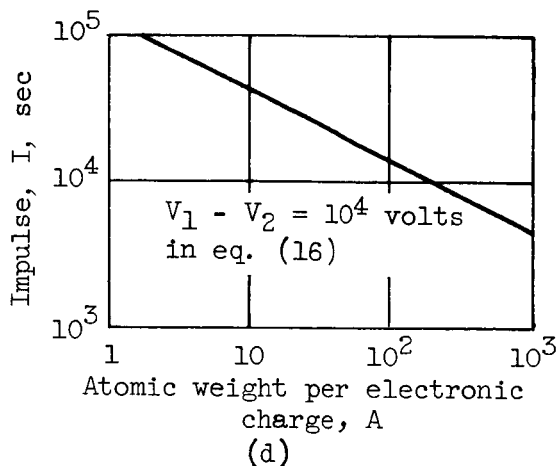
A practical design limit of mean electric field might be about  $10^7$  volts per meter. Equation (12) would then yield about 787 newtons per square meter of beam area (or about 80 kilograms/sq meter). Such a thrust-to-area ratio would be quite adequate for space propulsion - if it could be obtained for all impulses and particle weights. Unfortunately, minimum manufacturing tolerances may prevent full utilization of the dielectric strength of an insulator or vacuum. An approximate minimum electrode spacing of about  $10^{-3}$  meter might be expected from manufacturing tolerance limitations. With a spacing of  $10^{-3}$  meter, acceleration potential differences of less than  $10^4$  volts would yield mean electric-field values below  $10^7$  volts per meter and, from equation (14) or (15), correspondingly lower thrust-to-area ratios.

Specific impulse. - The accelerator potential difference for the Child's law ion accelerator can be related to impulse and atomic weight per electronic charge by dividing the velocity equation (3) by the dimensional constant  $g$ :

$$I = 1.417 \times 10^3 \sqrt{\frac{V_1 - V_2}{A}} \quad (16)$$

For a round-trip Mars mission with a nuclear-electric powerplant reasonably advanced over the present technology, optimum impulses of 5000 to 10,000 seconds are indicated by reference 3. A satellite orbit adjustment might utilize an impulse as low as 1000 seconds, while a mission to the outer planets might require an impulse of 20,000 seconds or greater. The range of interest for impulses is therefore from about 1000 to over 20,000 seconds.

Sketch (d) shows the specific impulse as a function of ion atomic weight for an accelerating potential difference of  $10^4$  volts, which corresponds to a field of  $10^7$  volts per meter and a spacing of  $10^{-3}$  meter. Above the line, the design limit of  $10^7$  volts per meter can be used for the field, while below the line the minimum electrode spacing of  $10^{-3}$  meter is used. Also, the greater the distance below the line, the less the mean electric field and (from eq. (14)) the less the thrust per unit beam area. For atomic ions, the specific impulses desired for most space missions fall below the line in sketch (d); consequently, heavy atomic ions, or perhaps even heavy molecular ions, will be desirable for



maximizing thrust per unit beam area. The effect of operation below the line in sketch (d) can be shown numerically by substituting equation (16) into equation (13):

$$\frac{F_1}{S} = 1.955 \times 10^{-24} \frac{I^4 A^2}{(x_2 - x_1)^2} \quad (17)$$

Thus, the thrust-area ratio decreases as the fourth power of impulse below the line in sketch (d).

The values selected for maximum mean potential gradient and minimum electrode spacing in the foregoing discussion ( $10^7$  volts/meter and  $10^{-3}$  meter) cannot be considered as more than rough approximations. Different design compromises can change the effective limits for different operating conditions. It is valid to conclude, however, that heavy ions will be desirable for high thrust-to-area designs at all but the highest specific impulses. The accelerate-decelerate principle (to be discussed later) can be used to reduce, but not eliminate, the thrust-area penalties associated with light ions and low specific impulses.

Electron accelerator problems. - For neutralization the total electron-beam current must equal the total ion-beam current. If it is assumed that the electron and ion accelerators have the same length (limited by tolerances), a simple approximate equation can be derived to show the connection between the velocity ratio and beam area ratio of the ion and electron accelerators. The approximation results from ignoring thermal motion, which would probably be significant for electrons. From Child's law (eq. (9)),

$$\left[ S \beta \frac{(V_1 - V_2)^{3/2}}{(x_2 - x_1)^2} \right]_+ = J \approx \left[ S \beta \frac{(V_1 - V_2)^{3/2}}{(x_2 - x_1)^2} \right]_- \quad (18)$$

$$\frac{S_-}{S_+} \approx -i \frac{(V_1 - V_2)^{3/2}}{(V_1 - V_2_-)^{3/2}} + \left(\frac{m_-}{m_+}\right)^{1/2} \quad (19)$$

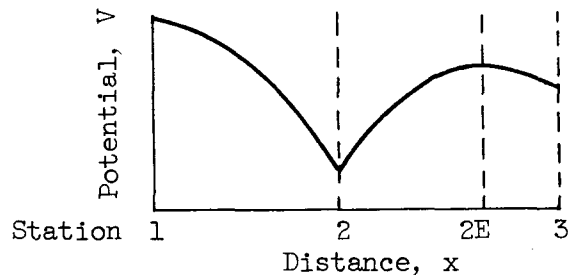
Substituting the velocity expression (eq. (3)) in (19) gives

$$\frac{S_-}{S_+} \approx \left(\frac{v_+}{v_-}\right)^3 \frac{m_+}{m_-} \quad (20)$$

For the same velocity and an ion atomic weight per charge of 100, the ratio of electron- to ion-beam area would be  $1.8 \times 10^5$ . The large weight implied by such a large beam area for the electron gun would be unacceptable. If, as an alternative approach, the ion-beam area is assumed the same size, the electron velocity would be 57 times that of the ions. As will be shown in the neutralization analysis, such a high electron velocity poses a problem. The accelerate-decelerate principle, however, helps to reduce both the electron velocity and the problem.

#### Internal Deceleration

Uniform initial velocity. - The internal deceleration region between stations 2 and 3 in an ion accelerator has the boundary condition of uniform but nonzero velocity at station 2. Again, the same boundary condition applies approximately to an electron accelerator for the same stations. A typical potential variation showing acceleration between stations 1 and 2 and deceleration between stations 2 and 3 is shown in sketch (e):



(e)

The sketch is shown for positive particles, but could be applied to negative particles merely by inverting the ordinate. A zero-electric-field plane, station 2E, is shown between stations 2 and 3, although it is also possible to have the zero-electric-field plane at station 2 or 3, or not in the region at all. The various possible locations of the zero electric field and the various potentials at that plane correspond

to a large number of solutions. A complete discussion of these solutions is not within the scope of this report. If the reader is interested in further details, references 5 and 7 are suggested.

The aim of this section is met if region 1 to 2 can be shown to be space-charge-limiting for current with the same spacing between 1 and 2 as between 2 and 3, so that the accelerate-decelerate accelerator can be analyzed by considering only the space-charge effects between stations 1 and 2. The current limitation of the station 1 to 2 region is demonstrated by showing a solution of the station 2 to 3 region that will carry more current than the 1 to 2 region with the same spacing. This particular solution uses the boundary values of a zero electric field, station 2E, between stations 2 and 3, with the particle velocity at station 2E equal to zero. Thus,

$$V_{2E} - V_2 = V_1 - V_2 \quad (21)$$

Also, there is no current reversal at station E, so that

$$j_2 = j_1 = j \quad (22)$$

Solving equation (4) for these boundary conditions,

$$\frac{j(x_3 - x_2)^2}{\beta(V_{2E} - V_2)^{3/2}} = \left[ 1 + \left( \frac{V_{2E} - V_3}{V_{2E} - V_2} \right)^{3/4} \right]^2 \quad (23)$$

Comparing equations (9) and (23) (note  $V_{2E}$  equals  $V_1$ ), it is evident that the left side of (23) can be considered as the ratio of current to that obtained from Child's law for the same potential difference and length. It is also evident that the ratio will be equal to or greater than unity. Reference 7 shows some solutions for the same ratio of  $(V_{2E} - V_3)/(V_{2E} - V_2)$ , but with  $V_{2E} \neq 0$ , that have even higher current ratios. But it will suffice here merely to note that, for the same distances between stations 2 and 3 as between 1 and 2, more current can be transmitted between stations 2 and 3. The dimensionless grouping on the left side of equation (23) is used throughout this report and is called the space-charge number.

Accelerate-decelerate. - An accelerator with an acceleration region followed by a deceleration region is called an A-D (accelerate-decelerate) accelerator. The deceleration may be internal or external (discussed in the section on external deceleration), although only the internal deceleration is considered here. For the same minimum spacing between stations 2 and 3 as between stations 1 and 2, beam current is determined by the electric field between stations 1 and 2. The impulse, as measured at station 3 (ignoring external space-charge effects), depends only on

the potential difference  $V_1 - V_3$ , so that a decrease in impulse will not change the current. Operation at impulses below the line in sketch (d) can thus be obtained without such a drastic reduction in thrust as the Child's law, or accelerate-only case. From equations (13) and (16), the thrust-area equation for the A-D accelerator is

$$\frac{F_i}{S} = 5.556 \times 10^{-15} \frac{E^{3/2} I \sqrt{A}}{\sqrt{x_2 - x_1}} \quad (24)$$

Comparing the A-D equation (24) with the Child's law equation (17) at a point on the curve of sketch (d), the same thrust-area ratio is obtained. This result should be expected because such a point for the A-D accelerator corresponds to no net deceleration from station 2 to 3. If the thrust-area ratios are compared at lower impulses, the Child's law values decrease as the fourth power of specific impulse, while the A-D values decrease by only the first power of specific impulse.

This thrust-area advantage of A-D ion accelerators over Child's law ion accelerators for low specific impulses, low ion weights, or both, was also shown in reference 4. The A-D system is not without losses, however, as some of the particles will strike the electrode at station 2. The resultant losses will be substantially independent of velocity at station 3 and hence will be a larger fraction of beam power as the final velocity is lowered.

The A-D principle has the further advantage for the ion accelerator of establishing a potential difference between stations 2 and 3 that would prevent electrons from going upstream to station 1. Sketch (e) shows an electric field at station 3 that would initially accelerate the electrons into the ion accelerator, but the electrons would not have sufficient energy to reach station 2 and they would merely turn around and go out again. As will be discussed in the section on the mixed electron-ion beam, collisions between ions and electrons can be neglected.

The A-D analysis also applies in approximate fashion to electron accelerators, so that higher beam current densities can be obtained with an A-D accelerator than with a Child's law accelerator with both having the same final velocity. Further discussion of the A-D principle as applied to electron accelerators, including thermal velocity effects, is presented in the next section.

#### Maxwellian Distribution

In this section the Maxwellian distribution is discussed first by itself and then as a boundary condition to solutions of Poisson's

equation for accelerators. Finally, the solutions of Poisson's equation with a Maxwellian distribution are discussed in their applications to accelerators.

A Maxwellian distribution of velocities in one dimension has the differential equation,

$$dn = \left( \frac{n_0}{\sqrt{\pi} \bar{v}} \right) e^{-(v'/\bar{v})^2} dv' \quad (25)$$

where  $dn$  is the number of particles in the velocity interval between  $v'$  and  $v' + dv'$ , and the most probable velocity  $\bar{v}$  is

$$\bar{v} = \sqrt{2kT/m} \quad (26)$$

To obtain the rate at which particles cross a unit area plane with a velocity greater than  $v'$ , equation (25) must be multiplied by the velocity of approach  $v'$  and integrated from  $v'$  to infinity, to obtain

$$\frac{\dot{n}}{S} = \left( \frac{n_0 \bar{v}}{2\sqrt{\pi}} \right) e^{-(v'/\bar{v})^2} \quad (27)$$

For charged particles, the potential expressions can be defined

$$V' = \frac{mv'^2}{2q} \quad (28)$$

and

$$\bar{V} = \frac{m\bar{v}^2}{2q} \quad (29)$$

which can be substituted for velocities. The flow rate of particles can be multiplied by the unit charge to obtain current density:

$$j = \frac{n_0 q^{3/2} \bar{v}^{1/2}}{(2\pi m)^{1/2}} e^{-V'/\bar{V}} \quad (30)$$

or simply

$$j = j_e e^{-V'/\bar{V}} \quad (31)$$

where the current  $j$  is the part of the emitted current  $j_e$  with a particle thermal potential greater in magnitude than  $V'$ . An alternative definition of mean thermal potential  $\bar{V}$  in terms of temperature is

$$\bar{V} = \frac{kT}{q} \quad (32)$$

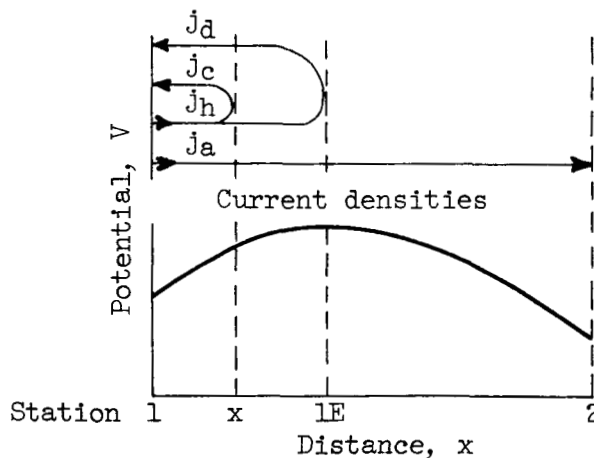
which, in mks units, is

$$\bar{V} = \pm 8.617 \times 10^{-5} T \quad (33)$$

Thus,  $11,605^\circ \text{ K}$  results in a mean thermal potential of 1 volt.

A Maxwellian distribution will be encountered with either a gaseous particle source or emission from a hot surface. For a gaseous particle source, such as a plasma, the Maxwellian distribution corresponds to the equilibrium condition. In practice, the equilibrium condition is reached quickly for electron-electron collisions and ion-ion collisions; hence, the Maxwellian distribution usually applies. Since equilibrium between electrons and ions is approached at a much slower rate, the electron and ion distributions may correspond to different temperatures. Emission of particles from a hot surface agrees both in theory and experiment with a Maxwellian distribution, as shown in references 8 to 10.

Acceleration region. - First consider the usual case where more current is emitted at station 1 than is transmitted to station 2. The potential variation in sketch (f) is again for positive particles, but would apply to negative particles if the potential variation were inverted:



The emitted current density  $j_e$  is equal to the sum of the current densities  $j_a$  and  $j_b$ , indicated in sketch (f). The transmitted current density  $j_t$  is simply  $j_a$ . The portion of the emitted current density with insufficient thermal energy to reach station  $1E$  reverses and returns to station 1, as shown by  $j_c$  and  $j_d$ . With a Maxwellian distribution of emitted particle energy, the current reversal process is, of course, continuous, and not stepwise as indicated in the sketch.

The charge density at any point  $x$  on the upstream side of station  $1E$  is obtained by integrating equation (6) over the total current density at that point. The total current density at point  $x$  in sketch (f), for example, would be  $j_a + j_b - j_c + j_d$ . Since the term  $j_c$  represents current that reversed before reaching point  $x$ , it was subtracted from  $j_b$ . It is convenient for calculation purposes to divide the current into downstream and upstream terms ( $j_a + j_b - j_c$ ) and  $j_d$  at point  $x$ . The sum of these terms thus represents the total current on the upstream side of station  $1E$ , while the difference represents the current  $j_t$  on the downstream side of station  $1E$ .

The differential current density, from equation (31), is

$$dj = -j_e e^{-V'/\bar{V}} dV'/\bar{V}$$

or, in terms of transmitted current,

$$dj = -j_t e^{(V_{1E} - V_1 - V')/\bar{V}} dV'/\bar{V} \quad (34)$$

Substituting equation (34) into (6),

$$\rho_q = \int_{V-V_1}^{\pm\infty} \frac{j_t e^{(V_{1E} - V_1 - V')/\bar{V}} dV'/\bar{V}}{\sqrt{2(V' - V + V_1)}(q/m)} \pm \int_{V-V_1}^{V_{1E}-V_1} \frac{j_t e^{(V_{1E} - V_1 - V')/\bar{V}} dV'/\bar{V}}{\sqrt{2(V' - V + V_1)}(q/m)} \quad (35)$$

In line with the discussion of sketch (f) the first term represents the downstream current and the second term the upstream current, with the integration limits determined accordingly. The  $+\infty$  is for positive particles, while the  $-\infty$  is for negative particles. The sum of the two terms of equation (35) represents the charge density on the upstream side of station  $1E$ , while the difference represents that on the downstream side.

Integrating (35) and substituting  $\alpha^2/2$  for  $(V' - V - V_1)/\bar{V}$  give

$$\rho_q = \frac{\sqrt{\pi} j_t e^{(V_{1E} - V)/\bar{V}}}{\sqrt{2\bar{V}}(q/m)} \left[ 1 \pm \sqrt{\frac{2}{\pi}} \int_0^{\sqrt{2(V_{1E} - V)/\bar{V}}} e^{-\alpha^2/2} d\alpha \right] \quad (36)$$

The positive sign in (36) is, of course, associated with the upstream side and the negative sign with the downstream side. The integrand in (36) can be readily evaluated from a table of the normal probability function, but only for specific values of  $(V_{1E} - V)/\bar{V}$ .

The charge density is used in Poisson's equation, but the integration must be numerical because equation (36) is evaluated from tables. Two equations that can be used for numerical solution of equation (1), Poisson's equation in one dimension, are

$$E = \pm \sqrt{-\frac{2}{\epsilon_0} \int_{V_{1E}}^V \rho_q dV} \quad (37)$$

and

$$x - x_{1E} = \pm \int_{V_{1E}}^V \frac{dV}{\sqrt{-\frac{2}{\epsilon_0} \int_{V_{1E}}^V \rho_q dV}} \quad (38)$$

Equation (38) cannot be evaluated by numerical integration for the interval from  $V_{1E}$  to  $(V_{1E} + \Delta V)$ , because there is a singularity at  $V_{1E}$ . The charge density varies slowly with potential close to  $V_{1E}$  and therefore may be assumed constant to integrate the denominator of (38). Equation (38) can then be integrated to obtain the first distance increment:

$$\Delta x = \pm \sqrt{-\frac{2\epsilon_0 \Delta V}{\rho_q}} \quad (39)$$

The procedure outlined is substantially that used by Langmuir in reference 11 for the case where more current is emitted than transmitted. For this case the ratio of local current to transmitted current on the upstream side is

$$j = j_{te}^{(V_{1E}-V)/\bar{V}} \quad (40)$$

On the downstream side the current is constant.

The results of reference 11, expressed in the parameters of this report, are presented in table I. The local and integrated charge density parameters in the table were calculated from equation (36) because they were not included in reference 11.

The tabulated results of reference 11 are plotted in figure 1 in terms of overall parameters that are more convenient for analysis and design. The nondimensional numbers used in figure 1 are the space-charge numbers based on both emitted and transmitted current and the ratio of mean thermal potential to the overall potential difference of the accelerator. Except for the case of zero thermal potential ratio, an increase in emitted current always causes an increase in transmitted current.

Also, unless emission-limited conditions are reached, an increase in mean thermal potential causes an increase in transmitted current. The zero thermal potential ratio agrees with Child's law, with the space-charge number based on transmitted current equal to unity.

The intercepts with the 45° line in figure 1 are for zero electric field at the emitter, which is for the limiting solution where  $j_e = j_t = j$ . An equation for these intercepts was obtained by Langmuir in reference 12 by taking the first two terms of a series expansion. That equation, with the constant changed slightly to give slightly better accuracy (within 1 percent) for values of  $\bar{V}/(V_1 - V_2)$  between zero and 10, is

$$\frac{j(x_2 - x_1)^2}{\beta(V_1 - V_2)^{3/2}} \cong 1 + 2.5 \sqrt{\frac{\bar{V}}{V_1 - V_2}} \quad (41)$$

Internal deceleration. - The boundary condition of a Maxwellian distribution of particle energy superimposed on a uniform initial velocity is used for the internal deceleration region. As in the previous case for internal deceleration, with uniform initial velocity, stations 1 and 2 will be current-limiting for the same spacing between 1 and 2 as between 2 and 3. This will be shown by again considering the boundary conditions of a zero electric field (station 2E) intermediate between stations 2 and 3 and a minimum particle velocity of zero at that station (station 2E). Equation (41) can thus be applied to the region between stations 2 and 2E:

$$\frac{j(x_{2E} - x_2)^2}{\beta(V_{2E} - V_2)^{3/2}} = 1 + 2.5 \sqrt{\frac{\bar{V}}{V_{2E} - V_2}} \quad (42)$$

Comparing (42) and (41), with the potential differences the same and the distance  $(x_{2E} - x_2)$  less than  $(x_2 - x_1)$ , it is evident that the current that region 2 to 3 can handle is greater than that for region 1 to 2.

An excess of emitted current over transmitted current would increase the transmitted current, as shown in figure 1. However, to increase the emitted current sufficiently to make the current capacity of region 1 to 2 greater than that of 2 to 3 is probably impractical with respect to particle-emission losses, and the region between stations 1 and 2 will probably be space-charge-limiting for the same distances between 1 and 2 as between 2 and 3.

Applications to accelerators. - The solutions with Maxwellian distributions as boundary conditions apply primarily to electron accelerators. The thermal potential of ions may be significant for some

low-specific-impulse applications, but generally it can be ignored. For example, ions with an atomic weight per charge of 100 coming from a source with a temperature as high as  $10,000^{\circ}$  K at a specific impulse of only 5000 seconds would have a ratio of thermal potential to accelerating potential difference of 0.0007. On the other hand, electrons coming from a surface as low as  $1000^{\circ}$  K at velocities corresponding to a specific impulse of 100,000 seconds would still have a thermal potential ratio of 0.03. In fact, a temperature of  $1000^{\circ}$  K without any accelerating potential difference is sufficient to give an average electron velocity equivalent to 15,000 seconds.

The A-D (accelerate-decelerate) principle is just as valid with a Maxwellian distribution for a boundary condition as with uniform velocity boundary condition, but is limited primarily to electron accelerators. In a manner completely analogous to the previous discussion with uniform initial velocity, the A-D principle permits higher current densities for the same final velocity. Electron impingement on the accelerating electrode and the space charge at the exit of the electron accelerator place practical limits on the use of the A-D principle, but it does represent a partial solution to the area-velocity compromise for electron guns discussed previously.

### External Deceleration

The external deceleration region is between the ion accelerator exit and the plane of electron injection. The electron-injection plane is not a true neutralization plane, as the neutralization process does not occur in a plane. There must be electric fields sufficient to distribute the electrons downstream of the electron-injection plane, although the magnitudes of these electric fields are negligible compared with those upstream. The solutions of the mixed electron-ion beam are presented in a later section of this report, but for this section the assumption of neutralization at the electron-injection plane and zero electric field downstream of that plane will be an adequate approximation of the real case.

The ion rocket exit is referred to as station 3 throughout this section, although it may actually be station 2. The electron-injection or neutralization plane is station N. Poisson's equation (eq. (1)) can be written

$$\frac{dE}{dx} = \frac{\rho}{\epsilon_0} \quad (43)$$

Thus, in passing from the downstream side of station N to the upstream side, there can be no finite change in electric field without a finite charge in the plane of N. Station N is assumed to be merely an

electron-injection plane without a physical electrode. Without an electrode, there can be no finite charge in the plane of N, and the electric fields upstream of station N must also be zero.

Uniform initial velocity. - Using the boundary condition of uniform initial velocity, equation (4) can be integrated. The first integration yields the electric field,

$$E = \sqrt{\frac{j}{\epsilon_0} \left( \frac{2m}{q} \right)^{1/2} \left( 2\sqrt{V_1 - V} - a \right)} \quad (44)$$

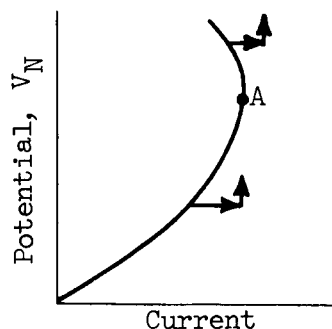
The constant of integration,  $a$ , is evaluated as  $2\sqrt{V_1 - V_N}$  from the additional boundary condition of  $E = 0$  at  $V = V_N$ . Integrating  $x$  between  $x_3$  and  $x_N$  and integrating  $V$  between  $V_3$  and  $V_N$  yields the solution

$$\frac{j(x_N - x_3)^2}{\beta(V_1 - V_3)^{3/2}} = 1 + 3 \left( \frac{V_1 - V_N}{V_1 - V_3} \right)^{1/2} - 4 \left( \frac{V_1 - V_N}{V_1 - V_3} \right)^{3/2} \quad (45)$$

Maxwellian distribution. - For the case of external deceleration with a Maxwellian energy distribution superimposed on the initial velocity, numerical integration is necessary. The potential differences are measured from the maximum value in the accelerator at station 1E. (If all the emitted current is being transmitted, the zero electric field is found at station 1, and station 1 is used instead of 1E for the potential difference.) The integration was accomplished with equation (38) with the potential integrated from  $V_N$  to  $V_3$  and the distance from  $x_N$  to  $x_3$ . The reverse direction was used to provide a zero electric plane as the starting point for the integration.

The solutions for the external deceleration region for a range of thermal potential ratios are plotted in figure 2. The curve for  $V/(V_{1E} - V_3) = 0$  was obtained from equation (45). The effect of increasing thermal potential ratio at all values of the potential ratio,  $(V_N - V_3)/(V_{1E} - V_3)$ , is to increase the space-charge number based on the difference  $V_{1E} - V_3$ . This result might be expected because an increase in thermal potential, with other parameters held constant, means an increase in average velocity at station 3.

An area of instability is revealed if all the parameters except current density and the potential at station N are assumed constant, as shown in sketch (g). A momentary increase in current will cause a transient departure from the equilibrium operation, as shown by the two horizontal arrows in sketch (g). The increased current will, after a



(g)

short time, increase the space charge between stations 3 and N. With  $V_3$  fixed, the increase in space charge will cause an increase in  $V_N$ , as shown by the two vertical arrows in sketch (g). Below the maximum current point A, the potential change offsets the initial current change by moving the operating point back towards the equilibrium line, and operation is stable. Above point A the converse is true. The potential change increases the initial departure from equilibrium due to the current change, and the operation is unstable.

The loci of the maximum space-charge numbers for the curves of figure 2 are shown by a dashed line. The region above this line is described as a region of possible instability. There is "possible instability" instead of just "instability" because stability depends on what parameters are allowed to vary in a particular physical situation, and the parameters assumed to vary in the preceding discussion may not be the ones actually encountered. For example, a physical electrode may be used at station N, and the zero electric field at station N may be desired as a boundary condition to prevent any electrons from going upstream of station N. The potential at N could then be fixed, instead of being permitted to vary, and there would be no instability region.

It should be pointed out that the external deceleration solution can be used for an A-D accelerator without a deceleration electrode, but the amount of deceleration in the A-D system must then be small enough to avoid instability. For negligible thermal potential, the final velocity at station N would have to be at least half the initial velocity to avoid this instability.

Only external deceleration of ions was considered to this point, but this solution may be applied approximately to electrons in the region between an electron-accelerator exit and the ion beam. The approximation

stems from the zero-electric-field assumption at station N. The electric fields of the mixing region are small compared with the ion electric fields upstream of N (as assumed), but may be quite significant as compared with the electric field upstream of a similar station N for electrons. Any application to electrons should therefore be made with care.

Thrust calculation. - The problems of calculating the thrust are associated with the external deceleration region, as will be shown by considering the magnitude of the various terms of the thrust equation. The general thrust equation for gases composed of charged particles has the usual hydrodynamic momentum and pressure terms plus the magnetic- and electric-field forces. The pressure term is negligible with particle densities of the order of  $10^{-9}$  atmosphere. The magnetic-field force term is negligible compared with the electric-field force term in the absence of an external magnetic field and relativistic particle velocities, which are not considered here. Also, the momenta of electrons are negligible compared with those of ions. The calculation of thrust reduces, then, to integration of ion-momentum forces and electric-field forces. The external region where both ion-momentum and electric-field forces are significant is between the exit of the ion accelerator and the electron-injection plane, which is the ion external deceleration region. For the simple one-dimensional case with both the velocity and electric field uniform over the area  $S$  at any station,

$$\frac{F}{S} = \frac{\dot{mv}}{S} - \frac{\epsilon_0 E^2}{2} \quad (46)$$

For further discussion of the thrust equation and the importance of the various terms, see reference 5.

For an example of thrust calculation, consider the case of external deceleration with uniform initial velocity. The first term is

$$\frac{\dot{mv}}{S} = j \sqrt{\frac{2m}{q}} \sqrt{v_1 - v} \quad (47)$$

The second term is obtained from equation (44):

$$\frac{\epsilon_0 E^2}{2} = j \sqrt{\frac{2m}{q}} \left( \sqrt{v_1 - v} - \sqrt{v_1 - v_3} \right) \quad (48)$$

Substituting equations (47) and (48) into (46),

$$\frac{F}{S} = j \sqrt{\frac{2m}{q}} \sqrt{v_1 - v_3} \quad (49)$$

Equation (49) demonstrates two things. First, the thrust force is independent of the plane of measurement as long as that plane is external

to hardware. Second, it is simpler to calculate the thrust at a plane where the electric field is zero.

For thrust calculation where appreciable ion thermal velocities are encountered, the ion-momentum term of equation (46) is replaced by the sum of particle momenta, which in turn equals the product of mass flow and average velocity:

$$\int \dot{m} \frac{v dm}{S} = \frac{\dot{m} v_{av}}{S} \quad (50)$$

Average velocity can be evaluated from

$$\frac{v_{av}}{\sqrt{2(V_{1E} - V)(q/m)}} = \int_0^\infty \sqrt{1 + \frac{V'}{V_{1E} - V_3}} e^{-V/\bar{V}} \frac{dV'}{\bar{V}} \quad (51)$$

Equation (51) was integrated numerically, and the following equation was obtained empirically:

$$\frac{v_{av}}{\sqrt{2(V_{1E} - V)(q/m)}} \approx 1 + 0.37 \left( \frac{\bar{V}}{V_{1E} - V} \right)^{3/4} \quad (52)$$

Equation (52) is accurate to about 1 percent for values of  $\bar{V}/V_3$  less than 10.

#### Mixed Electron-Ion Beam

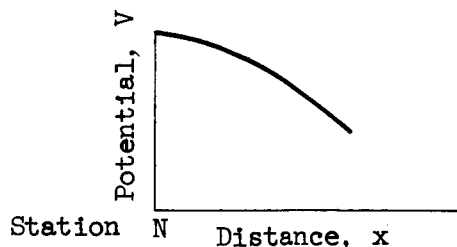
The difficulty in trying to match electron and ion accelerators was brought out in the section "Acceleration Region." The problem is primarily one of compromising electron-gun size with electron velocity, with both tending to be excessive, probably even with the A-D principle for the electron accelerator. The problem, then, is one of trying to slow the electrons after they are in the ion beam, so that the space charge of the electrons will neutralize that of the ions.

Various processes act to slow electrons in an ion gas, such as radiative recombination, bremsstrahlung, coulomb scattering, multiple ionization of ions, and electrostatic forces. For the impulse range of interest and probable particle density (assumed at  $10^{16}$  per cubic meter), only the electrostatic forces were significant. The lack of energy-dissipating processes means that the previous approach with Poisson's equation and the energy equation is adequate for mixed beams of ions and electrons. The purpose of this section is, of course, to determine the permissible electron velocity for neutralization.

Equal electron and ion currents. - The solution with uniform electron velocity and equal electron and ion currents uses equation (5). The ion-charge density is assumed constant, which is reasonable in view of the high mass of the ions compared with the electrons. To simplify the calculations, it is convenient to express the ion-charge density in terms of the electron charge and mass and the equivalent electron potential  $V_{eq}$ . The equivalent potential for an electron is that potential required to give ion velocity to the electron. Substituting the ion-charge-density expression in equation (5), and measuring potential difference from the minimum potential  $V_{min}$ , which will be shown to correspond to zero electron velocity, give

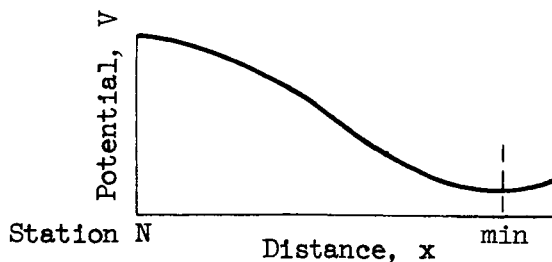
$$\frac{d^2V}{dx^2} = \frac{-j}{\epsilon_0 \sqrt{2(V_{min} - V_{eq})(q/m)}} \left( 1 - \sqrt{\frac{V_{eq} - V_{min}}{V - V_{min}}} \right) \quad (53)$$

To determine the integration limits of equation (53), some basic characteristics of Poisson's equation must be considered. If the electron accelerators have reasonable areas, then, in the region immediately downstream of station N, the electrons will have excess velocity over the ions, and the net charge density will be positive. From Poisson's equation, the potential variation with distance is concave downwards for a positive charge density. The maximum allowable electron velocity is obtained by placing the maximum of the potential curve at station N, as shown in sketch (h):



(h)

As the electrons go downstream, they slow down until the potential falls below the value required to give ion velocity, and the charge density becomes negative. The curve will then be concave upwards, as shown in sketch (i):



(i)

The maximum electron velocity at station N corresponds to the maximum potential at that point. The maximum potential at station N is, in turn, obtained with the lowest possible minimum downstream of station N. The lowest minimum potential corresponds to zero electron velocity, which agrees with the definition of potential difference used in equation (53). Thus, the maximum electron velocity at station N is obtained by integrating equation (53) over the range 0 to 0 for slope and  $V_{\min}$  to  $V_N$  for potential. Integrating and solving for the potential difference at station N,

$$V - V_{\min} = 4(V_{eq} - V_{\min}) \quad (54)$$

The maximum electron velocity at station N is therefore twice the ion velocity for the condition of equal-magnitude electron and ion currents, and occurs at a minimum electron velocity of zero. The potential variation shown in sketch (i) is cyclic with increasing distance. The wavelength can be calculated by integrating equation (53) twice. The wavelength turns out to be exactly the ion velocity divided by the plasma frequency, or

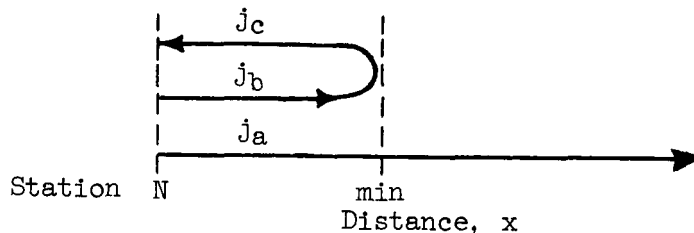
$$\lambda = \frac{\sqrt{2(V_{eq} - V_{\min})(-q/m)}}{\frac{1}{2\pi} \sqrt{\frac{(n_0 q^2)}{\epsilon_0 m}}} \quad (55)$$

The electron density  $n_0$  in equation (55) is the mean value between station N and the first minimum. Substituting mks values for constants and expressing (54) in terms of ion properties,

$$\lambda = 4.458 \times 10^{-11} v_+^{3/2} / j_+^{1/2} \quad (56)$$

The wavelengths calculated from equation (56) will generally be very small compared to hardware dimensions.

Electron current reversal. - If the electron velocity is greater than twice the ion velocity, only part of the emitted electron current passes beyond the first minimum. If only part of the electron current passes beyond the first minimum, then the ion beam will not be neutralized. An obvious possibility is increasing the electron current when the electron velocity is increased, so the electron current that escapes will be sufficient to neutralize the ion beam beyond the first minimum. The electron current for such a condition downstream of station N is shown in sketch (j):



(j)

The transmitted, emitted, and total electron currents are

$$j_{t,-} = j_a$$

$$j_{e,-} = j_a + j_b$$

$$j_{tot,-} = j_a + j_b + j_c$$

The method of solution is the same as the previous one, except the total electron current is used in the electron-charge term. The solution for maximum potential at station N is

$$V_N - V_{min} = 4(V_{eq} - V_{min}) \left( \frac{j_{tot}}{j_t} \right)^2_- \quad (57)$$

or, in terms of electron and ion velocities,

$$v_- = 2v_+ \left( \frac{j_{tot}}{j_t} \right) \quad (58)$$

Thus, the electron velocity may be much greater than the ion velocity if the total current is increased correspondingly. The returning electron current  $j_c$  may or may not be collected by an electrode. If  $j_c$  is merely reflected by electric fields in the ion accelerator, then the actual thermionic emission need be no larger than the transmitted current  $j_a$ . Even when all the returning electrons are collected and the electron accelerator must supply all downstream electrons, going to a higher electron velocity permits a reduction in electron accelerator exit area.

The length from station N to the first minimum is found to be larger than the half-wavelength given by equation (56) by the ratio  $j_{tot}/j_t$ . Downstream of the first minimum the wavelength would revert to that given by equation (55) or (56).

Maxwellian distribution. - The effect of a Maxwellian distribution of energies superimposed on electron velocities was also used as an initial boundary condition for the mixed-beam region. The solution was obtained by numerical integration of equation (37) from the first minimum to the maximum at station N. No net change of potential slope or electric field is involved; thus only the integration

$$\int_{V_{\min}}^{V_N} \rho_q dV$$

need be considered. Starting at the minimum, integration is continued until the value of the integral is zero, which is reached at  $V_N$ . The charge density  $\rho_q$  is the sum of the electron-charge density (from eq. (36)) and the ion-charge density (assumed constant because of the high ion-to-electron mass ratio). The solutions for a range of thermal potential ratios and total-to-transmitted current ratios were obtained and are plotted in figure 3.

The thermal potential ratio,  $-\bar{V}/(V_{eq} - V_{\min})$ , was limited to values less than  $\pi$ . For values greater than  $\pi$ , the integrated charge density for a Maxwellian distribution of electrons was less than the charge density of an equal-current-density ion beam, even with no accelerating potential difference. Thus, a solution with a neutralized beam is not possible for high thermal potential ratios. For the unity current ratio, the variation of maximum potential ratio,  $(V_N - V_{\min})/(V_{eq} - V_{\min})$ , is predicted within 0.15 by the approximate equation,

$$\frac{V_N - V_{\min}}{V_{eq} - V_{\min}} \approx \sqrt{1 - \left[ \frac{\bar{V}}{\pi(V_{eq} - V_{\min})} \right]^2} \quad (59)$$

The magnitude of potential effect is roughly the same at the other current ratios, so that percentagewise the thermal potential ratio is less important at high current ratios. Current ratios higher than unity in figure 3 were calculated for the case where all electrons returning to the ion accelerator are reflected by an electric field instead of collected by an electrode. The difference between the maximum electron potentials for either collection or reflection, however, is small for the same current ratio.

The limit of  $\pi$  for thermal potential ratio raises some practical questions, since it will be encountered in many proposed designs. The electron thermal energies are so small that even small dissipative processes may permit operation at thermal potential ratios substantially higher than  $\pi$ . The effective value determined from experiment may therefore depart considerably from  $\pi$ .

## SUMMARY OF RESULTS

Heavy ions are particularly desirable for high current density when ion-accelerator lengths are limited by manufacturing tolerances rather than dielectric strength. The A-D (accelerate-decelerate) principle also helps to offset the effect of minimum electrode spacing on ion current density.

The similar design of electron and ion accelerators leads to excessive electron velocities, exit areas, or both, probably even when the A-D principle is utilized for the electron accelerator. With excessive electron velocities, only part of the electron current goes downstream when neutralization is attempted. High electron velocities can be utilized, however, if the total electron current is large enough that the electron current transmitted is sufficient to neutralize the ion beam.

Since the high-electron-velocity mixed-beam solutions are accompanied by upstream electron currents, the ion accelerator must be able to withstand electrons bombarding the exit. The A-D principle is also useful for preventing harm to the ion accelerator due to this electron bombardment, because the electrons will be unable to pass through the field of the accelerating electrode and reach the ion source.

A possible limit on neutralization is imposed by thermal motion of electrons. The analysis indicated an upper limit for the temperature of the electron source for each value of specific impulse, although the thermal potentials involved are small and the analytical results may not agree with experimental findings.

Lewis Research Center

National Aeronautics and Space Administration  
Cleveland, Ohio, November 2, 1959

## REFERENCES

1. Oberth, Hermann: Das elektrische Raumschiff. Ch. 22 of Wege zur Raumschiffahrt, 1929, pp. 409-423.
2. Stuhlinger, E.: Possibilities of Electrical Space Ship Propulsion. Extract from Proc. Fifth Int. Astronautical Cong., 1954, pp. 109-119.
3. Moeckel, W. E.: Propulsion Methods in Astronautics. Paper presented at Int. Cong. Aero. Sci., Madrid (Spain), Sept. 8-13, 1958.

4. Childs, J. H.: Design of Ion Rockets and Test Facilities. Paper No. 59-103, Inst. Aero. Sci., 1959.
5. Mirels, Harold, and Rosenbaum, Burt M.: Analysis of One-Dimensional Ion Rocket with Grid Neutralization. NASA TN D-266, 1960.
6. Child, C. D.: Discharge from Hot Lime. Phys. Rev., vol. 32, 1911, pp. 492-511.
7. Spangenberg, Karl Ralph: Vacuum Tubes. McGraw-Hill Book Co., Inc., 1948.
8. Compton, Karl T., and Langmuir, Irving: Electrical Discharges in Gases. I - Survey of Fundamental Processes. Rev. Modern Phys., vol. 2, no. 2, Apr. 1930, pp. 123-130.
9. Cohen, V. W., and Ellett, A.: Velocity Analysis by Means of the Stern-Gerlach Effect. Phys. Rev., vol. 52, Sept. 1937, pp. 502-508.
10. Jeans, James: An Introduction to the Kinetic Theory of Gases. Cambridge Univ. Press (London), 1952.
11. Langmuir, Irving: The Effect of Space Charge and Initial Velocities on the Current Between Parallel Plane Electrodes. Phys. Rev., vol. 21, 1923, p. 419.
12. Langmuir, Irving, and Compton, Karl T.: Electrical Discharges in Gases. II - Fundamental Phenomena in Electrical Discharges. Rev. Modern Phys., vol. 3, no. 2, Apr. 1931, pp. 191-257.

TABLE I. - CHARGE AND CURRENT PARAMETERS FOR A MAXWELLIAN DISTRIBUTION OF INITIAL VELOCITIES

(a) Emission side

$\frac{V_{1E} - V_1}{\bar{V}}$	$\frac{\rho_q}{J_t} \sqrt{\frac{2V_q}{m}}$	$\int \frac{V_{1E} - V_1}{\bar{V}} \frac{\rho_q}{J_t} \sqrt{\frac{2V_q}{m}} \frac{dV}{\bar{V}}$	$\frac{j_t^{1/2}(x_{1E} - x_1)}{\beta^{1/2} \bar{V}^{3/4}}$	$\frac{j_e}{j_t}$	$\frac{V_{1E} - V_1}{\bar{V}}$	$\frac{\rho_q}{J_t} \sqrt{\frac{2V_q}{m}}$	$\int \frac{V_{1E} - V_1}{\bar{V}} \frac{\rho_q}{J_t} \sqrt{\frac{2V_q}{m}} \frac{dV}{\bar{V}}$	$\frac{j_t^{1/2}(x_{1E} - x_1)}{\beta^{1/2} \bar{V}^{3/4}}$	$\frac{j_e}{j_t}$
0	1.772	0	0	1.000	2.1	28.36	23.69	1.626	8.166
.01	1.992	.019	.162	1.010	2.2	31.42	26.68	1.648	9.025
.02	2.095	.040	.219	1.020	2.3	34.80	29.99	1.668	9.974
.05	2.326	.106	.341	1.051	2.4	38.52	33.65	1.686	11.02
.10	2.635	.230	.473	1.105	2.5	42.64	37.70	1.704	12.18
.15	2.916	.369	.571	1.162	2.6	47.19	42.19	1.721	13.46
.20	3.189	.522	.651	1.221	2.7	52.22	47.15	1.737	14.88
.25	3.460	.688	.719	1.284	2.8	57.77	52.65	1.752	16.44
.30	3.736	.868	.780	1.350	2.9	63.91	58.73	1.764	18.17
.35	4.017	1.061	.834	1.419	3.0	70.69	65.45	1.780	20.09
.40	4.307	1.270	.883	1.492	3.1	78.19	72.89	1.793	22.20
.45	4.607	1.492	.928	1.568	3.2	86.47	81.12	1.805	24.53
.50	4.917	1.730	.970	1.649	3.3	95.62	90.21	1.816	27.11
.55	5.240	1.984	1.009	1.733	3.4	105.7	100.3	1.827	29.96
.60	5.577	2.254	1.045	1.822	3.5	116.9	111.4	1.837	33.12
.65	5.927	2.542	1.080	1.916	3.6	129.3	123.7	1.847	36.60
.70	6.294	2.847	1.112	2.014	3.7	142.9	137.3	1.856	40.45
.75	6.677	3.171	1.142	2.117	3.8	156.0	152.3	1.865	44.70
.80	7.077	3.515	1.171	2.226	3.9	174.7	168.9	1.873	49.40
.85	7.496	3.879	1.199	2.340	4.0	193.1	187.3	1.881	54.60
.90	7.936	4.265	1.225	2.460	4.5	318.7	312.6	1.916	90.02
.95	8.396	4.673	1.250	2.586	5.0	525.7	519.4	1.942	148.4
1.0	8.878	5.105	1.274	2.718	5.5	867.0	860.5	1.962	244.7
1.1	9.315	6.044	1.319	3.004	6.0	1,428.	1,423.	1.979	403.4
1.2	11.06	7.091	1.361	3.320	6.5	2,357.	2,351.	1.991	665.1
1.3	12.31	8.259	1.400	3.669	7.0	3,887.	3,880.	2.001	1,096.
1.4	13.70	9.558	1.435	4.055	7.5	6,409.	6,402.	2.008	1,808.
1.5	15.23	11.00	1.468	4.482	8.0	10,566.	10,559.	2.014	2,981.
1.6	16.91	12.61	1.499	4.953	8.5	17,422.	17,414.	2.019	4,915.
1.7	18.77	14.39	1.528	5.474	9.0	28,724.	28,716.	2.022	8,103.
1.8	20.83	16.37	1.555	6.050	9.5	47,359.	47,351.	2.025	13,360.
1.9	23.09	18.56	1.580	6.686	10.	78,081.	78,073.	2.027	22,026.
2.0	25.60	21.00	1.604	7.389	1000.	-----	-----	2.035	-----

TABLE I. - CONCLUDED. CHARGE AND CURRENT PARAMETERS FOR A  
MAXWELLIAN DISTRIBUTION OF INITIAL VELOCITIES

(b) Transmission side

$\frac{V_{1E} - V_2}{\bar{V}}$	$\frac{\rho_q}{J_t} \sqrt{\frac{2V_q}{m}}$	$\int_0^{\frac{V_{1E}-V_2}{\bar{V}}} \frac{\rho_q}{J_t} \sqrt{\frac{2V_q}{m}} \frac{dV}{\bar{V}}$	$\frac{J_t^{1/2}(x_2 - x_{1E})}{\beta^{1/2} \bar{V}^{3/4}}$	$\frac{V_{1E} - V_2}{\bar{V}}$	$\frac{\rho_q}{J_t} \sqrt{\frac{2V_q}{m}}$	$\int_0^{\frac{V_{1E}-V_2}{\bar{V}}} \frac{\rho_q}{J_t} \sqrt{\frac{2V_q}{m}} \frac{dV}{\bar{V}}$	$\frac{J_t^{1/2}(x_2 - x_{1E})}{\beta^{1/2} \bar{V}^{3/4}}$
0	1.772	0	0	7.0	0.3553	3.874	6.003
.01	1.589	.016	.156	7.5	.3445	4.049	6.269
.02	1.522	.032	.231	8.0	.3347	4.219	6.530
.05	1.401	.076	.371	8.5	.3256	4.384	6.786
.10	1.283	.143	.533	9.0	.3173	4.545	7.037
.15	1.202	.205	.661	9.5	.3095	4.705	7.284
.20	1.141	.263	.771	10.	.3023	4.854	7.526
.25	1.091	.319	.869	11.	.2893	5.150	8.000
.30	1.049	.372	.959	12.	.2779	5.434	8.461
.35	1.013	.424	1.044	13.	.2677	5.706	8.911
.40	.9812	.474	1.123	14.	.2586	5.969	9.350
.45	.9529	.522	1.198	15.	.2503	6.224	9.779
.50	.9273	.569	1.270	16.	.2428	6.470	10.20
.55	.9040	.615	1.339	17.	.2359	6.707	10.61
.60	.8827	.660	1.405	18.	.2296	6.942	11.02
.65	.8131	.702	1.470	19.	.2238	7.169	11.42
.70	.8449	.746	1.532	20.	.2184	7.390	11.81
.75	.8280	.788	1.592	25.	.1962	8.423	13.70
.80	.8122	.829	1.651	30.	.1797	9.361	15.48
.85	.7974	.869	1.709	35.	.1667	10.23	17.17
.90	.7835	.908	1.765	40.	.1562	11.03	18.80
.95	.7703	.947	1.820	45.	.1475	11.79	20.37
1.0	.7579	.985	1.874	50.	.1400	12.51	21.89
1.1	.7349	1.060	1.979	55.	.1336	13.19	23.37
1.2	.7140	1.132	2.080	60.	.1280	13.85	24.81
1.3	.6951	1.202	2.178	65.	.1231	14.47	26.22
1.4	.6775	1.271	2.274	70.	.1187	15.08	27.60
1.5	.6614	1.338	2.367	75.	.1147	15.66	28.95
1.6	.6465	1.404	2.457	80.	.1111	16.23	30.28
1.7	.6325	1.468	2.545	85.	.1078	16.82	31.58
1.8	.6195	1.530	2.632	90.	.1048	17.31	32.87
1.9	.6074	1.592	2.717	95.	.1021	17.82	34.14
2.0	.5959	1.652	2.800	100.	.09951	18.33	35.38
2.1	.5851	1.711	2.882	110.	.09492	19.30	37.82
2.2	.5749	1.769	2.963	120.	.09091	20.23	40.20
2.3	.5652	1.826	3.042	130.	.08735	21.12	42.53
2.4	.5560	1.882	3.120	140.	.08422	21.98	44.82
2.5	.5473	1.937	3.197	150.	.08138	22.80	47.07
2.6	.5390	1.991	3.272	160.	.07881	23.60	49.28
2.7	.5312	2.045	3.346	170.	.07647	24.38	51.45
2.8	.5236	2.098	3.420	180.	.07433	25.13	53.58
2.9	.5163	2.150	3.493	190.	.07230	25.87	55.68
3.0	.5093	2.201	3.565	200.	.07054	26.58	57.75
3.1	.5026	2.252	3.636	250.	.06312	29.91	67.72
3.2	.4962	2.301	3.706	300.	.05764	32.92	77.18
3.3	.4901	2.351	3.776	350.	.05338	35.70	86.23
3.4	.4841	2.400	3.845	400.	.04994	38.27	94.95
3.5	.4784	2.448	3.913	450.	.04708	40.70	103.4
3.6	.4729	2.495	3.981	500.	.04468	42.99	111.6
3.7	.4676	2.542	4.048	550.	.04259	45.17	119.6
3.8	.4625	2.589	4.114	600.	.04079	47.25	127.4
3.9	.4575	2.635	4.179	650.	.03921	49.25	135.0
4.0	.4527	2.680	4.244	700.	.03777	51.18	142.5
4.5	.4308	2.901	4.562	750.	.03649	53.03	149.9
5.0	.4118	3.111	4.868	800.	.03533	54.83	157.1
5.5	.3952	3.313	5.163	850.	.03428	56.57	164.2
6.0	.3804	3.507	5.451	900.	.03331	58.26	171.2
6.5	.3672	3.694	5.730	950.	.03243	59.90	178.1
				1000.	.03161	61.50	184.9

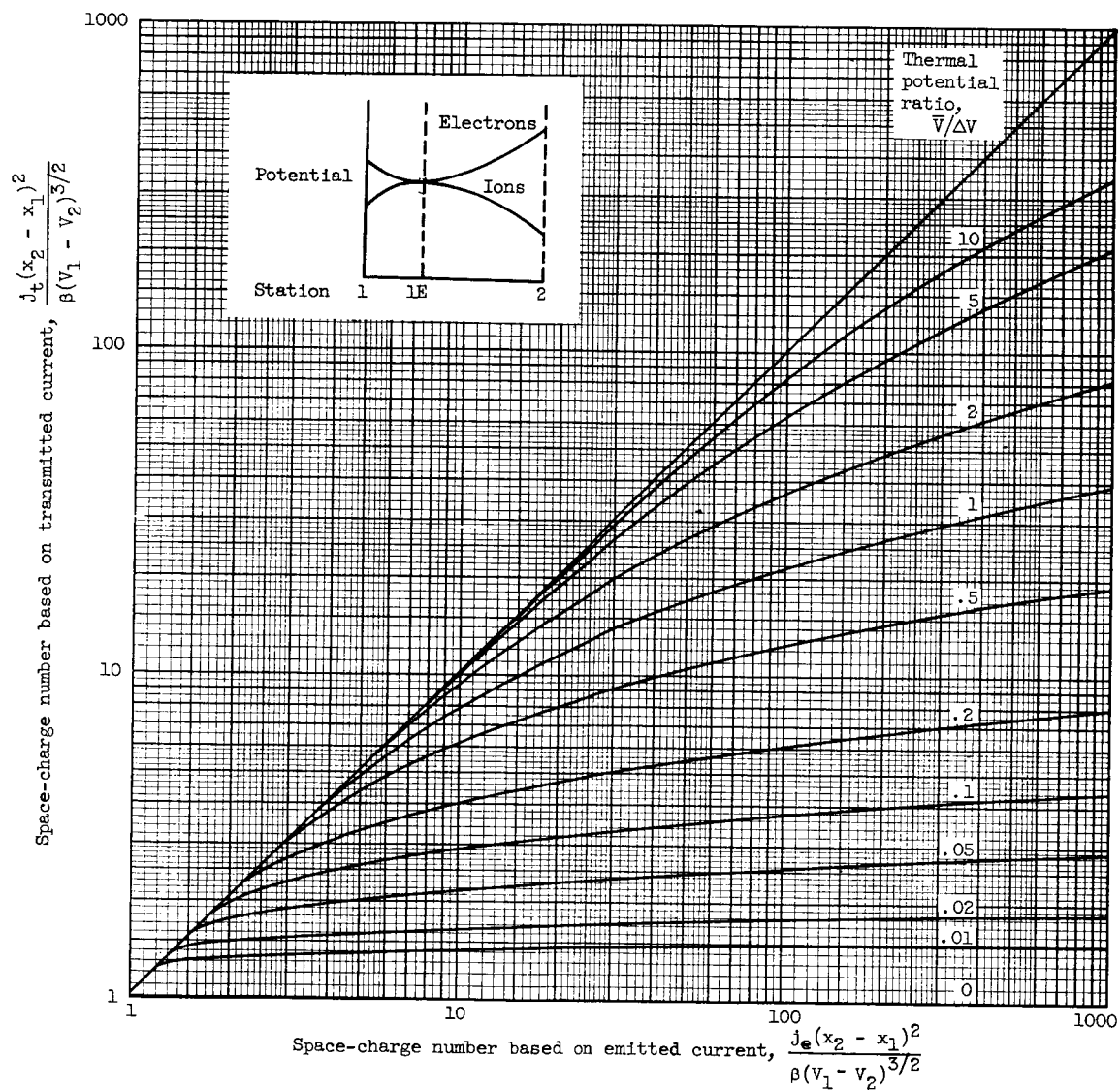


Figure 1. - Solutions for the acceleration region with an initial Maxwellian velocity distribution of emitted particle velocities.

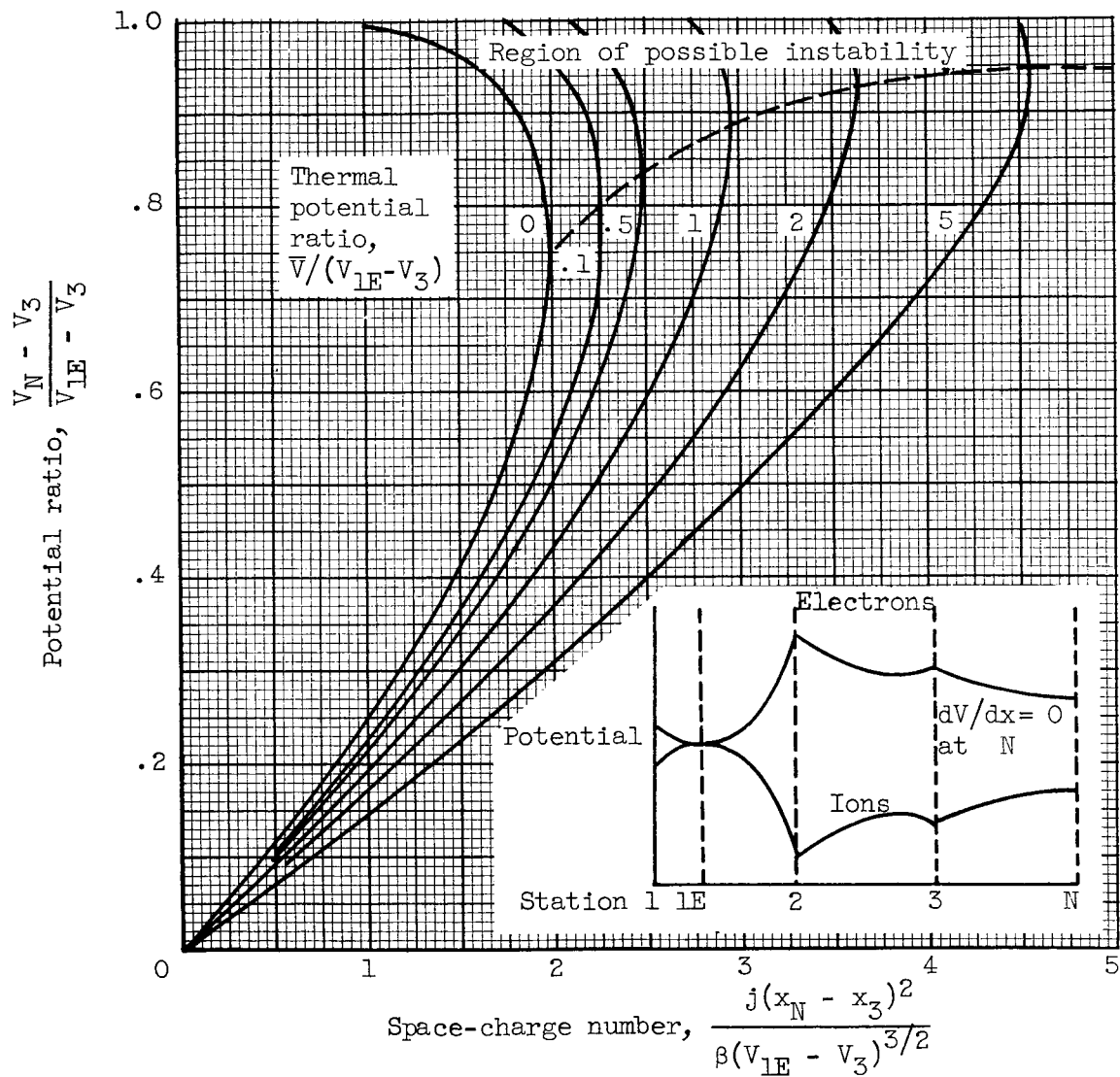


Figure 2. - External deceleration solutions with zero electric field at neutralization plane.

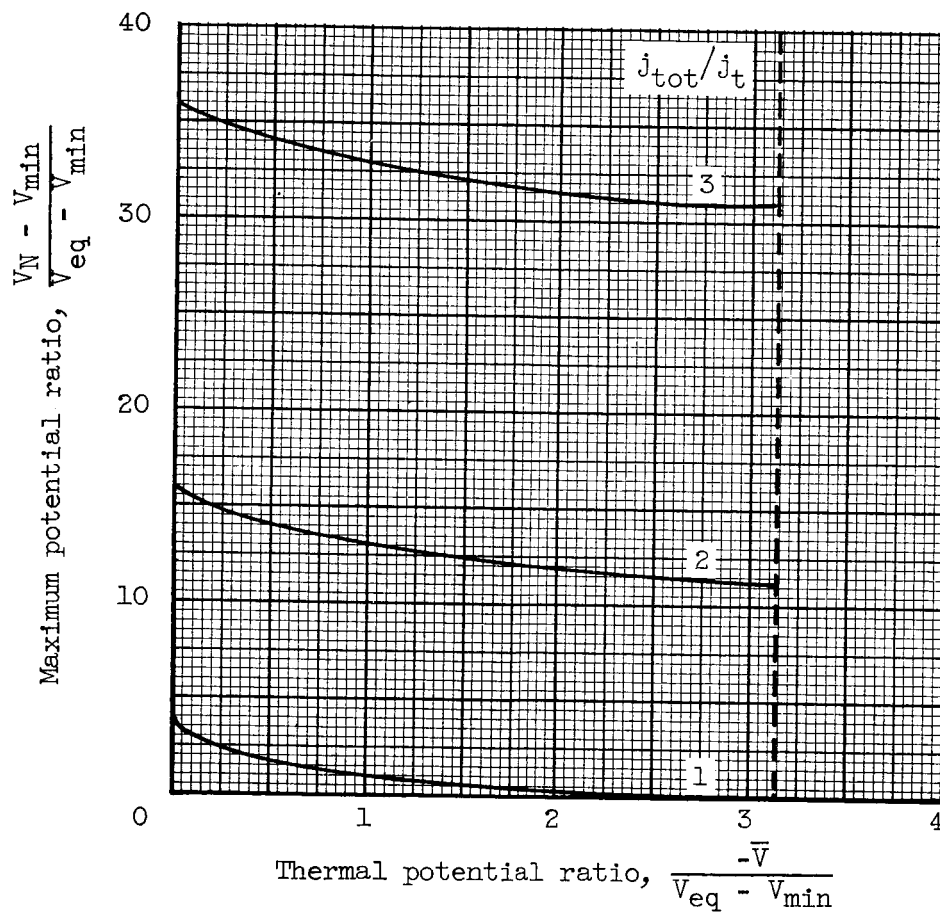


Figure 3. - Ratio of maximum electron potential difference to ideal potential difference as function of thermal potential ratio for a mixed electron-ion beam.